A&A 430, 303–311 (2005)
DOI: 10.1051/0004-6361:20041440

Astronomy & Astrophysics

Mg II chromospheric radiative loss rates in cool active and quiet stars

D. Cardini

Istituto di Astrofisica Spaziale e Fisica Cosmica, CNR, via del Fosso del Cavaliere 100, 00133 Roma, Italy
e-mail: cardini@rm.iasf.cnr.it

Received 9 June 2004 / Accepted 14 September 2004

Abstract. The Mg II *k* emission line is a good indicator of the level of chromospheric activity in late-type stars. We investigate the dependence of this activity indicator on fundamental stellar parameters. To this purpose we use *IUE* observations of the Mg II *k* line in 225 late-type stars of luminosity classes I–V, with different levels of chromospheric activity. We first re-analyse the relation between Mg II *k* line luminosity and stellar absolute magnitude, performing linear fits to the points. The ratio of Mg II surface flux to total surface flux is found to be independent of stellar luminosity for evolved stars and to increase with decreasing luminosity for dwarfs. We also analyse the Mg II *k* line surface flux-metallicity connection. The Mg II *k* emission level turns out to be not dependent on metallicity. Finally, the Mg II *k* line surface flux-temperature relation is investigated by treating separately, for the first time, a large sample of very active and normal stars. The stellar surface fluxes in the *k* line of normal stars are found to be strongly dependent on the temperature and slightly dependent on the gravity, thus confirming the validity of recently proposed models. In contrast, data relative to RS CVn binaries and BY Dra stars, which show very strong chromospheric activity, are not justified in the framework of a description based only on acoustic waves and uniformly distributed magnetic flux tubes so that they require more detailed models.

Key words. stars: late-type – stars: chromospheres – stars: activity – ultraviolet: general – line: profiles

1. Introduction

The Mg II *h* and *k* resonance lines as well as the Ca II *H* and *K* lines have played and continue to play an important role in the understanding of physical conditions in the chromospheres of late-type stars. In particular the Mg II emission lines, which are formed at higher temperatures and greater heights than the Ca II lines, are important tools for the diagnosis of chromospheric properties and, thanks to the large abundance of Magnesium, are good indicators of the total chromospheric radiative loss (Linsky & Ayres 1978). In addition, the photospheric background around the region of 2800 Å being small or negligible compared to the chromospheric flux, the problem of photospheric background subtraction is considerably reduced with respect to Ca II.

For all these reasons, Mg II emission lines have been widely studied both in the Sun and in late-type stars (Basri & Linsky 1979; Cerruti-Sola et al. 1992; Mathioudakis & Doyle 1992; Elgarøy et al. 1997; Buchholz et al. 1998).

The presence of resonance emission lines in late type stars is generally attributed to chromospheric temperature gradients generated by nonradiative heating (Ayres 1979). Two different types of mechanisms have been identified as responsible for chromospheric heating: hydrodynamic (acoustic and pulsational waves) and magnetic mechanisms (Narain & Ulmschneider 1996; Buchholz et al. 1998; Ulmschneider et al. 2001; Fawzy et al. 2002a).

The heating by acoustic waves appears to be the basic mechanism generating a *basal* flux strongly dependent on the colour of the star, but independent of luminosity class (Oranje & Zwaan 1985; Schrijver 1987; Rutten et al. 1991).

The fact that stars with the same fundamental stellar parameters, like effective temperature, luminosity, and metallicity show a broad range of chromospheric activity is generally attributed to different fractions of the stellar surface covered by magnetic fields (Rutten et al. 1991; Baliunas et al. 1995). Indeed, high-resolution observations of the Sun show considerable spatial variation in Mg II fluxes which become larger in regions of higher magnetic activity.

Several semiempirical and theoretical models of stellar chromospheres have been proposed (see Ayres 1979; Ulmschneider et al. 2001; Fawzy et al. 2002a). Theoretically predicted *basal* emission fluxes are in good agreement with minimal observed emission fluxes. On the other hand, the modeling of magnetic surface structure, which is responsible for the *excess* flux, roughly accounts for the observed line emission fluxes in Ca II, but does not explain the large emission fluxes in Mg II (Buchholz et al. 1998; Fawzy et al. 2002b).

Article published by EDP Sciences and available at http://www.aanda.org or http://dx.doi.org/10.1051/0004-6361:20041440

To test our understanding of the generation, propagation and dissipation of both mechanical and magnetical energy fluxes, it is useful to provide an empirical estimate of the amount of chromospheric heating in a large sample of stars covering a wide range of stellar properties.

In this paper we present the results of the analysis of the Mg II k λ 2796.34 Å emission line of 225 stars, with spectral type F6–M 6 and luminosity class I–V, as measured from a large number (more than 1400) of *IUE* spectra. Our sample contains stars with different level of activity, namely dwarfs, very active main sequence stars like BY Dra, giants and supergiants, and RS CVn, chromospherically active evolved stars.

The interest of our analysis mainly lies in the following points:

1. The method used to measure intensities of lines is the same for a very large sample of different types of stars.
2. The absolute flux scale is the same for all our stars and is accurate due to the use of high precision measurements of distances.
3. The effective temperatures and bolometric corrections have been determined fron $B-V$ colours using unique accurate numerical relations.

The paper is organized as follows. In Sects. 2 and 3 we describe our sample of stars, the *IUE* observations and their reduction to absolute surface flux units. In Sect. 4 we search for trends of estimated chromospheric radiative loss rates with basic parameters of stars such as effective temperature $T_{\rm eff}$, luminosity and metallicity. In Sect. 5 we compare our observations to avalaible theoretical models and our conclusions are given in Sect. 6.

2. Sample of stars

The data base used in the present paper was generated starting from the original sample of 230 normal stars used in a study of the Wilson-Bappu effect by Cassatella et al. (2001) (hereafter Paper I). It was a sample of stars with good quality Mg II observations from *IUE* (see Sect. 3) and known parallaxes from *HIPPARCOS* with luminosity classes ranging from I to V. Since for the purpose of the present paper we need accurate determination of spectral type, colour and bolometric correction, we have further selected the original sample in order to avoid indetermined spectral classification, large errors on $B-V$ (>0.1) and too large bolometric corrections (<−2.3) (see Sect. 3) because they are too uncertain. We obtained a final sample of 173 nominally quiet stars.

In addition to normal stars, we consider here a sample of 29 very active evolved stars of the RS CVn type. They have been selected following the criteria given in Cardini et al. (2003) (hereafter Paper II) and further selected following the criteria illustrated above.

Finally, we added a sample of BY Dra stars wich consist of both single and binary dwarf stars having strong Ca II H and K emission lines. We have included all objects appearing as BY Dra stars in the SIMBAD data base for which *IUE* high resolution long-wavelength spectra and *HIPPARCOS* parallaxes were available. As selection criteria, we have adopted the same as Papers I and II and described above. These constitute our sample of 23 chromospherically active main sequence stars with spectral types F to K.

The resulting sample (225 stars) consists of an accurately selected, uniformly reduced and homogeneously calibrated data set.

3. Observations and data processing

The spectroscopic Mg II observations have been obtained with the *IUE* high resolution long wavelength camera. The calibrated spectra have been analysed and processed in order to obtain the Mg II k emission line strength using the method described in Paper II, which consists of a direct integration of the observed profiles, as measured above the photospheric flux level. As stars in our sample all have parallaxes measured astrometrically, they all are nearby stars. This makes us confident that the interstellar absorbtion can be neglected. On the other hand the evaluation of the interstellar absorbtion requires information which is usually lacking. The estimated relative uncertainty in the derivations of the apparent flux from observations is ±15%. In the case of binaries with two emitting stars (three known objects between BY Dra and five between RS CVn) we have not deblended both contributions. Indeed AR Lac is the only target in our sample in which the individual contribution from the two stars is evident as a consequence of their similar Mg II luminosity and of the favorable inclination angle of the system. Due to the statistical character of the present investigation, we have not considered it necessary to perform a detailed analysis of these spectra so that the integrated flux of both componets is considered.

In our data sample there are stars that have been observed two or more times. Some active stars have been observed hundreds of times. In all these cases a mean value of the flux was computed.

The apparent visual magnitudes of all stars along with their luminosity class, $B-V$, trigonometric parallaxes and the relative errors were obtained mostly from the *HIPPARCOS* catalogue. In a few cases, mainly regarding RS CVn and BY Dra stars, information on colour and luminosity class was taken from the Strasbourgh Data Center (SIMBAD) or from the recent literature. We have assumed a typical error of ±0.01 mag on visual magnitudes.

To convert fluxes at Earth, f, into stellar surface fluxes, F, we have used the following relation:

$$\log{(F/f)} = 0.350 + 4\ \log\ T_{\rm eff} + 0.4(V + BC) \qquad (1)$$

where $T_{\rm eff}$ is the effective temperature and BC the bolometric correction both derived from $B-V$ colour using the coefficients to the polinomial fits given by Flower (1996); V is the apparent visual magnitude. The constant 0.350 is derived from the solar values given by Allen (1983). The uncertainty on the chromospheric surface fluxes resulting from this conversion is hardly evaluable and the cooler the stars the larger the uncertainty. For binaries, we used combined values of $B-V$; in this way a further error in the calculation of surface fluxes is introduced. To prevent too large uncertainties in BC we have limited our sample to $B-V < 1.7$ which corresponds to $BC \approx -2.3$.

Table 1. Mg II k line fluxes for BY Dra stars. For each object we give the Hipparcos number, the star name, the spectral type and luminosity class, the reference for spectral type, the $B-V$ color index, the absolute visual magnitude, the log of the surface Mg II k flux, the metallicity, and the indication of binarity. For objects with double-lined spectra, the last column indicates which one of the stellar components is the active star.

HIP	Name	Sp. type	Ref.	$B-V$	M_V	log $F_{\rm Mg\,II}$	[Fe/H]	bin	Active star
1803	BE Cet	G4 V	1	0.66	4.84	6.15	−0.01		
11964	CC Eri	K7 V/M3 V	2	1.39	8.58	6.35	–	*	
16537	ε Eri	K2 V	3	0.88	6.18	6.04	−0.09		
19855	V891 Tau	G6 V	3	0.68	5.34	6.28	–		
19934	V984 Tau	K0 V	4	0.81	5.59	6.12	–		
20237	V986 Tau	G0 V	4	0.56	4.20	6.30	–		
20485	V989 Tau	K5 V	4	1.23	7.09	5.86	–		
20553	V895 Tau	G1 V	4	0.60	4.32	6.36	–		
20719	V906 Tau	G1 V	4	0.65	4.73	6.20	–		
20815	V993 Tau	F8 V	4	0.54	4.11	6.16	–		
20890	V918 Tau	G8 V	4	0.74	5.14	6.38	–		
20899	V920 Tau	G2 V	4	0.61	4.45	6.23	–		
21482	V833 Tau	K3 IV	3	1.10	6.84	6.40	–	*	
30630	OU Gem	K3 V/K5 V	5	0.94	5.95	6.32	–	*	Both
46816	LQ Hya	K2 V	2	0.93	6.50	6.31	–		
46843	DX Leo	G9 V	3	0.78	5.80	6.28	–		
57269	V838 Cen	K1 V/K2 V	2	0.91	5.47	6.33	–	*	Both
71631	EK Dra	G5 V	3	0.63	4.95	6.53	–		
72659	37 Boo	G7 V	3	0.72	5.41	6.22	−0.15		
81300	V2133 Oph	K0 V	3	0.83	5.82	5.90	0.01		
82588	V2292 Oph	G8 V	3	0.75	5.51	6.25	–		
83601	V2213 Oph	F9 V	3	0.58	4.45	6.07	−0.19		
91009	BY Dra	K4 V/K7.5 V	5	1.27	7.12	6.25	–	*	Both

Notes: (1) Cutispoto et al. (2003); (2) Cutispoto (1998); (3) Gray et al. (2003); (4) Strasbourgh Data Center (SIMBAD); (5) Catalog of Active Binary Stars (CABS) by Strassmeier et al. (1993).
The last two columns are according to CABS except for V838 Cen (see Cutispoto 1998).

Information on metallicity ([Fe/H]) could be found only for a subsample of 130 quiet stars and few very active stars (see Carney et al. 1994; Cayrel et al. 1997).

Tables 1 and 2 give the Mg II k logarithmic surface fluxes, together with other relevant data, for BY Dra and RS CVn stars respectively. Similar information is provided in Table 3 for normal stars. Units for the Mg II surface fluxes F are in erg cm^{-2} s^{-1}.

4. Discussion of the observations

In this Section we investigate the dependence, if any, of the chromospheric radiative loss rates on fundamental stellar parameters such as luminosity, metallicity, and temperature.

4.1. Line intensity-luminosity relation

In Fig. 1 we have plotted the logarithm of the Mg II k line absolute luminosity against absolute magnitude for normal stars (Fig. 1a) and active stars (Fig. 1b). Also indicated are the linear fits to the data for, separately, evolved (crosses) and main sequence (open squares) normal stars. To simplify the figures, error bars are not reported. In the figure are also drawn, for comparison, the "average" Mg II k luminosity for quiet solar regions, the "average" Mg II k luminosity for plage areas and the Mg II k luminosity in the flare of September 5, 1973, as reported by Cerruti-Sola et al. (1992) (filled circles).

Figure 1a clearly shows that the dependence of the line intensity on the stellar luminosity is different for evolved and dwarf normal stars. A least-squares fit to the data of normal evolved stars (class I–IV) provides:

$$\log L_{\rm Mg\,II} = (30.32 \pm 0.01) - (0.45 \pm 0.01)\, M_V \quad (2)$$

with a correlation coefficient of 0.95. The slope coefficient of about −0.4 in Eq. (2) suggests that for giants and supergiants the Mg II line intensity is directly proportional to stellar luminosity.

A similar fitting procedure applied to normal dwarf stars gives:

$$\log L_{\rm Mg\,II} = (30.07 \pm 0.04) - (0.29 \pm 0.01)\, M_V \quad (3)$$

with a correlation coefficient of 0.82. The slope coefficient smaller than in Eq. (2) indicates that dwarf stars have an excess of Mg II k luminosity which increases with increasing magnitude.

Equation (2) is in very good agreement with the result of Weiler & Oegerle (1979) based on stars brighter than $M_V = 4$ but it is quite different from our fit in Paper II because this last was performed on the whole sample of dwarfs and giants together. Other authors (e.g. Linsky & Ayres 1978;

Table 2. Mg II k line fluxes for RS CVn stars. For each object we give the Hipparcos number, the star name, the spectral type and luminosity class, the orbital period, the $B-V$ color index, the absolute visual magnitude, the log of the surface Mg II k flux, and the metallicity. For objects with double-lined spectra, the last column indicates which one of the stellar components is the active star.

HIP	Name	Sp. type	P_{orb}(days)	$B-V$	M_V	log $F_{Mg II}$	[Fe/H]	Active star
4157	CF Tuc	G0 V/K4 IV	2.8	0.68	2.93	6.82	–	Cool
9630	XX Tri	K0 III	24.0	1.11	1.92	6.74	–	
10280	TZ Tri	F5/K0 III	14.7	0.77	0.08	6.36	–	Cool
13118	VY Ari	K3-4 V-IV	13.2	0.96	3.72	6.53	–	
16042	UX Ari	G5 V/K0 IV	6.4	0.88	2.96	6.78	–	Cool
16846	V711 Tau	G5 IV/K1 IV	2.8	0.88	3.51	6.84	–	Both
19431	EI Eri	G5 IV	1.9	0.71	3.28	6.73	–	
23743	BM Cam	K0 III	80.9	1.11	−0.33	6.37	–	
35600	AR Mon	G8 III/K2-3 III	21.2	1.06	1.52	6.39	–	Both
37629	σ Gem	K1 III	19.6	1.12	1.36	6.36	–	
46159	IL Hya	G8 V/K0 III-IV	12.9	1.01	1.96	6.53	–	Cool
56851	V829 Cen	G5 V/K1 IV	11.7	0.95	2.44	6.57	–	
59600	HU Vir	K0 IV	10.4	0.97	3.21	6.63	–	
59796	DK Dra	K1 III/K1 III	64.4	1.15	0.59	6.33	–	Both
65187	BM CVn	K1 III	20.6	1.16	2.08	6.41	–	
82080	ε UMi	A8-F0 V/G5 III	39.5	0.90	−0.92	5.99	–	Cool
84586	V824 Ara	G5 IV/K0 V-IV	1.7	0.80	4.38	6.89	–	Both
85852	DR Dra	WD/K0-2 III	905.9	1.04	1.54	6.31	–	Cool
94013	V1762 Cyg	K1 IV-III	28.6	1.09	1.65	6.40	–	
95244	V4138 Sgr	K1 III	13.0	1.03	2.00	6.39	–	
96003	V1817 Cyg	A2 V/K2 III-II	108.8	1.12	−1.17	6.36	–	Cool
96467	V1764 Cyg	F-K1 III:	40.1	1.22	0.45	6.33	–	
109002	HK Lac	F1 V/K0 III	24.4	1.05	1.02	6.57	–	Cool
109303	AR Lac	G2 IV/K0 IV	2.0	0.76	2.99	6.51	−0.70	Both
111072	V350 Lac	K2 III	17.7	1.17	0.97	6.03	–	
112997	IM Peg	K2 III-II	24.4	1.13	0.93	6.43	–	
114639	SZ Psc	F8 IV/K1 IV	4.0	0.79	2.67	6.71	–	Cool
116584	λ And	G8 III-IV	20.5	0.98	1.75	6.48	−0.56	
117915	II Peg	K2-3 V-IV	6.7	1.01	4.38	6.68	–	

Notes: Spectral types and orbital periods are from the Catalog of Active Binary Stars (CABS) by Strassmeier et al. (1993) except for IL Hya (see Weber & Strassmeier 1998).
The last Column is according to CABS except for TZ Tri and IL Hya (see Montes et al. 1995 and Fekel et al. 1999 respectively).

Weiler & Oegerle 1979; Basri & Linsky 1979) report, on the basis of a sample mainly containing giant and supergiant stars and only few dwarfs, that the ratio of the Mg II flux rate to stellar luminosity is not dependent on stellar luminosity. On the basis of the present analysis, we confirm that this is true only for evolved stars but is not true for main sequence stars.

As far as very active stars are concerned, we show in Fig. 1b the location of RS CVn + BY Dra in the (log $L_{Mg II}$, M_V) diagram. We can notice that there is a good correlation between the logarithmic Mg II k line intensity and M_V for RS CVn stars (pluses). A fit to these data gives:

$$\log L_{Mg II} = (31.46 \pm 0.04) - (0.33 \pm 0.01)\, M_V \quad (4)$$

with $r = 0.94$.

Figure 1b also shows that BY Dra stars (diamonds) have a slope similar to that of normal main sequence stars. However, the coefficients of the fit are not reported here given the quite low data correlation ($r = 0.74$).

The mean activity level of RS CVn stars is comparable to that of an intense solar flare (about 1.3 dex greater than the level of quiet Sun) and that the activity level of BY Dra stars may be as large as that of solar plages (the mean run exceeds by 0.6 dex the quiet Sun).

4.2. Flux-metallicity relation

In Fig. 2 is plotted the logarithm of the Mg II k surface flux as a function of metallicity, for the 130 stars for which this latter parameter is known. The figure shows clearly that, in spite of the large range of metallicity covered, the radiative losses from the Mg II k line do not show any correlation with chemical abundance. This is true also considering evolved (crosses) and main sequence stars (open squares) separately. The figure shows also that main sequence stars have greater surface fluxes than evolved stars with the same metallicity, thus confirming the higher level of activity of these stars as already pointed out in Sect. 4.1.

Due to the scarcity of the metallicity data available (see Tables 1 and 2), a similar analysis has not been attempted for BY Dra and RS CVn stars.

Table 3. Mg II *k* line fluxes for normal stars. For each star we give the Hipparcos number, the spectral type and luminosity class, the $B-V$ color index, the absolute visual magnitude, the log of the surface Mg II *k* flux, and the metallicity.

HIP	Sp. type	$B-V$	M_V	log $F_{\mathrm{Mg\,II}}$	[Fe/H]	HIP	Sp. type	$B-V$	M_V	log $F_{\mathrm{Mg\,II}}$	[Fe/H]
544	K0 V	0.75	5.39	6.10	–	31592	K0 III	1.04	2.46	5.20	.05
1562	K2 III	1.21	−1.18	4.88	−.09	32768	K0 III	1.21	−0.80	4.79	–
2021	G2 IV	0.62	3.45	5.26	−.23	33817	K1 V	0.88	5.89	5.93	–
2081	K0 III	1.08	0.52	5.14	–	34622	K0 III	1.02	0.86	5.18	–
3092	K3 III	1.27	0.81	4.71	.04	35264	K3 I	1.62	−4.92	4.48	–
3093	K0 V	0.85	5.65	5.45	−.17	35907	K0 III	1.25	−1.51	4.96	.06
3179	K0 II	1.17	−1.99	4.96	−.09	37379	K3 III	1.54	−1.61	4.23	−.22
3419	K0 III	1.02	−0.30	5.50	.13	37447	K0 III	1.02	0.71	4.95	−.09
3765	K2 V	0.89	6.38	5.50	−.29	37740	G8 III	0.93	0.35	5.13	−.16
3821	G0 V	0.59	4.59	5.60	−.31	37826	K0 III	0.99	1.09	5.10	−.04
4422	G8 III	0.96	0.62	5.05	−.51	38170	G6 I	1.22	−4.74	5.31	.24
5364	K2 III	1.16	0.68	4.88	.04	40526	K4 III	1.48	−1.22	4.38	−.24
5447	M0 III	1.58	−1.86	4.63	−.10	41704	G4 II	0.86	−0.40	5.28	−.21
6537	K0 III	1.07	0.87	4.96	−.22	41926	K0 V	0.78	5.95	5.58	–
6867	K5 II	1.54	−0.87	4.82	–	42673	K0 III	0.96	−0.35	5.57	–
7607	K3 III	1.27	−0.04	4.67	.00	42808	K2 V	0.92	6.35	6.08	–
7884	K3 III	1.35	−0.81	4.48	−.24	43813	G8 III	0.98	−0.21	5.08	.38
8102	G8 V	0.73	5.68	5.48	−.66	44700	G8 I	1.04	−2.03	5.46	.38
9884	K2 III	1.15	0.48	4.95	−.21	44897	F9 V	0.58	4.54	5.77	–
10644	G0 V	0.61	4.66	6.05	−.30	45860	M0 III	1.55	−1.02	4.58	−.26
12114	K3 V	0.92	6.50	5.42	–	46390	K3 III	1.44	−1.69	4.61	−.12
12444	F6 V	0.52	4.12	5.95	.02	46404	G2 V	0.64	2.91	5.62	−.31
13701	K1 III	1.09	0.83	4.98	−.23	47193	K3 III	1.49	−3.31	4.64	.09
14135	M2 III	1.63	−1.61	4.26	–	47908	G0 II	0.81	−1.46	5.59	.17
14668	K0 III	0.98	1.11	5.11	.04	48455	K0 III	1.22	0.83	4.91	.12
15474	M3 III	1.61	−0.79	4.68	–	50583	K0 III	1.13	−0.92	4.43	−.49
16134	K5 V	1.34	7.89	5.74	–	51172	K4 III	1.43	−0.97	4.72	−.39
17440	K0 IV	1.13	1.41	4.92	–	52727	G5 III	0.90	−0.06	5.81	–
17678	M2 III	1.59	−0.83	4.61	–	53229	K0 III	1.04	1.41	4.61	−.20
18543	M1 III	1.59	−1.19	4.52	–	53721	G0 V	0.62	4.29	5.39	.01
19335	F7 V	0.52	3.87	6.24	–	53740	K1 III	1.08	0.44	4.98	−.22
19747	K1 III	1.09	1.07	4.99	–	54539	K1 III	1.14	−0.27	4.91	−.13
19921	K2 IV	1.08	3.13	5.01	–	55282	K0 III	1.11	−0.32	5.05	−.48
20205	G8 III	0.98	0.28	5.44	.13	57439	G0 II	0.89	−1.51	5.57	–
20455	G8 III	0.98	0.41	5.23	.06	57757	F8 V	0.52	3.40	5.88	.13
20850	K0 V	0.84	5.66	6.08	–	58576	K0 IV	0.76	4.99	5.55	.16
20885	G7 III	0.95	0.42	5.54	.04	59316	K2 III	1.33	−1.82	4.20	−.13
20889	K0 III	1.01	0.14	5.04	.04	60172	K1 III	1.17	0.26	5.18	−.48
20917	K7 V	1.36	8.00	5.70	–	60260	K3 III	1.39	−0.63	4.74	–
22263	G3 V	0.63	4.87	6.19	−.13	61084	M4 III	1.60	−0.56	4.62	–
22449	F6 V	0.48	3.67	6.05	.02	61359	G5 II	0.89	−0.51	5.30	.27
23123	K2 II	1.37	−2.86	4.67	.26	63090	M3 III	1.57	−0.57	4.72	−.09
26366	G8 III	0.95	1.33	5.38	−.53	64022	K5 III	1.48	−0.04	4.43	−.26
27628	K1 III	1.15	1.01	4.89	.13	64394	G0 V	0.57	4.42	5.91	.03
27750	K2 II	1.38	−2.91	4.87	−.25	64792	G0 V	0.58	3.92	6.35	.10
27890	K1 III	1.02	2.47	4.90	.10	64962	G8 III	0.92	−0.05	5.20	.06
27913	G0 V	0.59	4.70	6.47	−.03	65721	G5 V	0.71	3.68	5.25	−.11
29696	G8 III	1.02	0.75	5.15	−.33	67275	F7 V	0.51	3.54	6.06	.00
30343	M3 III	1.62	−1.39	4.43	–	67457	M5 III	1.52	0.51	4.96	–
31205	K0 III	1.10	0.88	5.34	−.42	68815	M6 III	1.24	0.68	4.47	–

Table 3. continued.

HIP	Sp. type	$B-V$	M_V	log $F_{\rm Mg\,II}$	[Fe/H]	HIP	Sp. type	$B-V$	M_V	log $F_{\rm Mg\,II}$	[Fe/H]
68933	K0 III	1.01	0.70	5.05	.03	90496	K1 III	1.02	0.95	5.11	−.20
70692	K4 III	1.43	−0.87	4.72	−.16	91117	K2 III	1.32	0.21	4.62	−.18
71053	K4 III	1.30	0.27	4.88	−.17	92043	F6 V	0.48	2.79	5.97	−.11
71681	K1 V	0.90	5.70	5.59	.26	92761	K1 II	1.41	−3.91	5.06	–
71683	G2 V	0.71	4.34	5.37	.15	92791	M4 III	1.58	−2.98	4.79	–
72010	K3 III	1.36	0.07	4.70	–	92862	M5 III	1.40	−1.07	5.25	–
72370	K5 III	1.43	−1.67	4.46	–	93864	K1 III	1.17	0.48	5.02	−.23
73184	K4 V	1.02	6.86	5.64	.01	94376	G9 III	0.99	0.63	5.09	−.27
74395	G8 III	0.92	0.65	5.09	–	94713	K0 II	1.26	−2.51	4.92	.28
74666	G8 III	0.96	0.69	5.23	−.26	95822	K0 III	1.05	0.85	4.89	−.08
76423	M5 II	1.20	0.50	5.56	–	97433	G8 III	0.89	0.59	5.23	−.18
77070	K2 III	1.17	0.87	4.70	−.05	98110	K0 II	1.02	0.74	5.09	−.09
79882	G8 III	0.97	0.64	5.05	−.01	99461	K2 V	0.87	6.41	5.50	−.58
80331	G8 III	0.91	0.58	5.20	−.21	100437	K0 II	1.08	0.06	5.25	.00
80704	M6 III	1.29	−0.39	5.14	.02	101474	K2 I	1.59	−2.66	4.60	–
80816	G8 III	0.95	−0.50	4.41	−.27	101772	K0 III	1.00	0.65	5.03	.03
81065	G9 IV	0.92	0.41	5.62	−.05	102422	K0 IV	0.91	2.63	5.27	−.32
81833	G8 III	0.92	0.80	5.45	−.18	102488	K0 III	1.02	0.76	5.06	−.18
82273	K2 II	1.45	−3.62	4.89	−.06	103227	K0 III	1.25	−2.66	5.15	−.06
82396	K2 III	1.14	0.78	4.92	−.17	104060	K5 I	1.61	−4.07	4.54	−.45
84345	M5 II	1.16	−2.57	5.55	–	105090	K7 V	1.40	8.71	5.49	–
84380	K3 II	1.44	−2.10	4.62	−.18	105406	F8 V	0.53	4.27	6.25	−.13
85068	G8 III	0.99	0.27	5.37	–	106642	M4 III	1.34	−0.43	4.21	–
85258	K3 I	1.48	−3.49	5.02	.50	107089	K0 III	1.01	2.10	5.21	–
85670	G2 II	0.95	−2.43	5.98	.14	107119	K0 III	1.11	0.89	4.90	.04
86742	K2 III	1.17	0.76	4.84	.00	107472	K0 I	1.38	−2.41	5.46	.06
87158	G5 IV	0.94	1.27	5.68	–	108870	K5 V	1.06	6.89	5.79	−.23
87261	K0 III	1.19	0.24	4.87	–	109492	K1 I	1.56	−3.35	4.81	.22
87585	K2 III	1.18	1.06	4.92	−.09	109937	K3 III	1.45	−2.28	4.48	−.12
87808	K1 II	1.35	−2.70	4.96	−.24	110130	K3 III	1.39	−1.05	4.63	–
87933	G8 III	0.94	0.61	5.62	−.10	112724	K0 III	1.05	0.76	5.03	.02
88048	G9 III	0.99	−0.03	4.93	.16	112748	G8 III	0.93	0.74	5.07	−.03
88601	K0 V	0.86	5.50	5.96	−.05	112961	M2 III	1.63	−1.67	4.53	–
88839	G7 III	0.94	−0.59	5.13	–	113881	M2 II	1.65	−1.49	4.25	−.11
88972	K2 V	0.88	6.15	5.54	−.20	114971	G7 III	0.92	0.68	5.20	−.44
89962	K0 III	0.94	1.84	5.18	−.42	116727	K1 IV	1.03	2.51	5.20	.04
90139	K2 III	1.17	0.87	4.93	−.16						

Units for the Mg II surface fluxes F are in erg cm^{-2} s^{-1}.

4.3. Flux-colour relation

In Fig. 3 we have plotted the observed surface fluxes in the Mg II *k* line versus $B-V$ for normal stars (Fig. 3a) and active stars (Fig. 3b).

In Fig. 3a we notice that:

- The observed minimum fluxes of giant (crosses) and supergiant (triangles) stars decrease with decreasing temperature.
- The observed minimum flux level of supergiants (class I–II) is a factor of two larger in $F_{\rm Mg\,II}$ compared to giant stars of the same colour.
- Surface fluxes of luminosity class V stars (open squares) are only weakly dependent on temperature, if not all. It is difficult for these stars to identify a line of minimum fluxes as they are sparsely distributed with a spread of about one order of magnitude at high temperatures.

As for stars with known very active chromospheres shown in Fig. 3b we observe that:

- RS CVn binaries (pluses) lie far above typical stars as seen before (Sect. 4.1). Minimum fluxes for these stars are well represented by the line of minimum fluxes defined by giants enhanced by a factor as large as 20.
- BY Dra stars (diamonds) lie 0.6 dex above normal main squence stars. Their observed fluxes do not show any dependence on temperature.

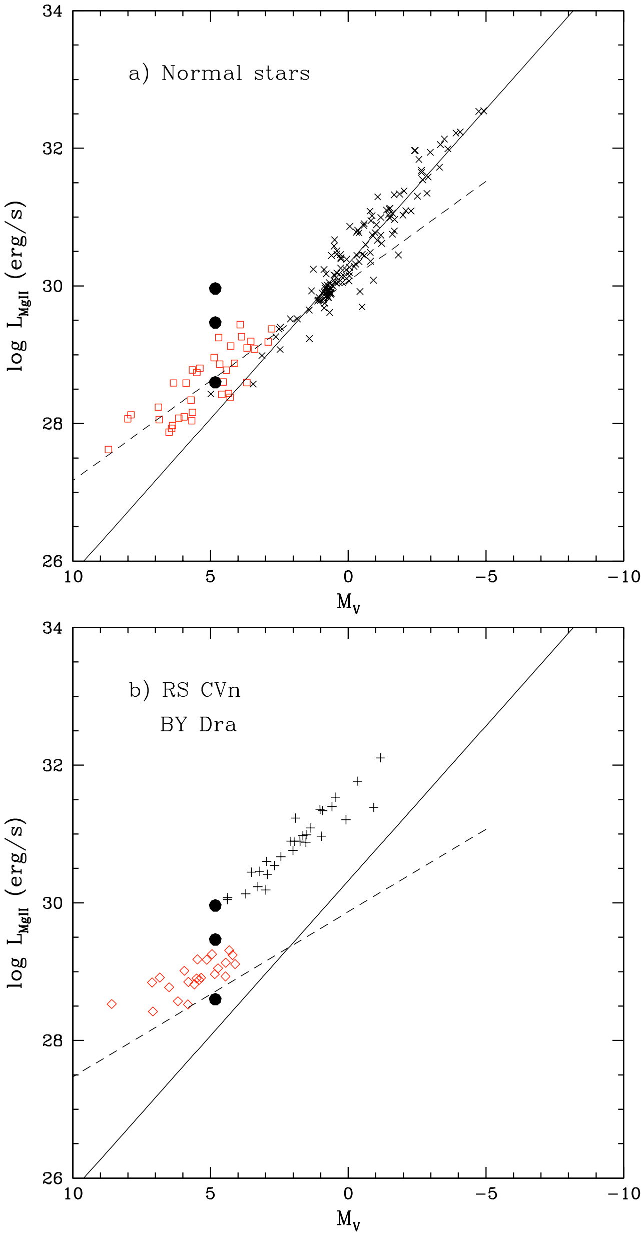

Fig. 1. The logarithmic absolute luminosity in the Mg II k line is plotted as a function of the absolute visual magnitude. **a)** Quiet stars. Dwarfs are shown as open squares and evolved stars as crosses. **b)** RS CVn (pluses) and BY Dra stars (diamonds). The best fits to the data of normal stars are represented for dwarfs by a dashed line and for giants by a full line. For comparison also data of the Sun are reported as filled circles (see text).

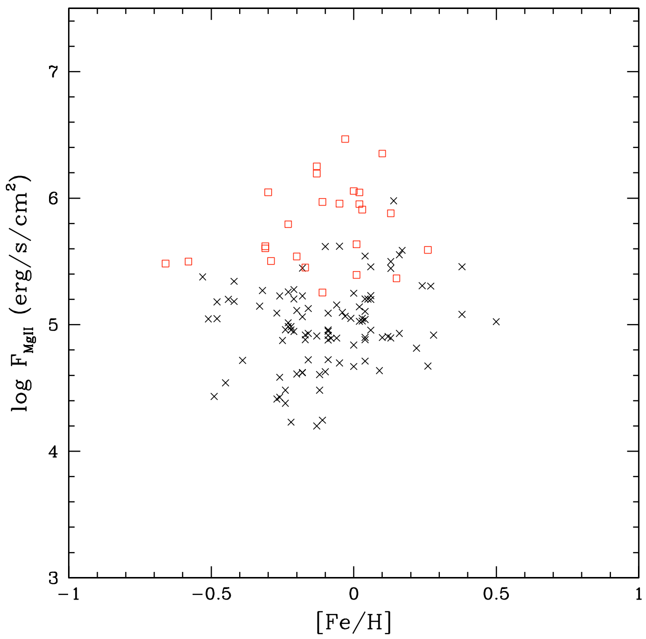

Fig. 2. The logarithm of the surface flux in the Mg II k line is plotted as a function of metallicity for a subsample of 130 stars. Open squares indicate main sequence stars and crosses indicate evolved stars.

5. Interpretation of the results

In Fig. 3 we compare our observational determination of Mg II k line fluxes at stellar surfaces with the simulated estimates of the same quantities computed by Fawzy et al. (2002b) using two-component models of stellar chromospheres for late-type main sequence stars. The dashed line refers to fluxes computed taking into account pure acustic wave heating only (*basal* fluxes). In addition to this mechanism the models predict an increase in Mg II emission due to magnetic tube waves proportional to the fraction of the stellar surface covered by magnetic fields (filling factor) (Fawzy et al. 2002a). The solid curve in Fig. 3 refers to a magnetic filling factor of 0.4 which corresponds to maximum efficiency in magnetic wave heating and then determines the upper boundary of the chromospheric activity. Figure 3a also shows the observational minimum limits from Rutten et al. (1991) (dotted line). All the quoted curves have been decreased by a factor of two to consider the k line only.

Buchholz et al. (1998) have simulated chromospheric Mg II minimum emission fluxes both for main sequence stars and giants concluding that they are essentially the same. Thus, minimum fluxes computed by Fawzy et al. (2002b) for dwarf stars can be considered valid also for giants. The existence of such a common lower boundary in the surface flux versus colour is strongly supported by the observations of the Ca II and Mg II lines (Schrijver 1987; Mathioudakis & Doyle 1992; Rutten et al. 1991; Fawzy et al. 2002b).

The Ca II theoretical low and upper emission boundaries agree with the observations within a factor of two, which is justified given the inaccuracies in the model and/or by uncertainties in observed flux determinations. For Mg II, Fawzy et al. (2002b), comparing their theoretical emission fluxes with observational fluxes given by Rutten et al. (1991), concluded that the modeled minimum flux limit was within a factor of two compatible with observations, but, even taking a factor of two uncertainty into account, the upper limit obtained was persistently lower than the maximum observed emission.

Looking at our data in Fig. 3a we see that our observational minimum limit is well defined in the range of $B-V$ between 0.85 and 1.5, where numerous giant stars (class III) are present. This limit is in good agreement with the line of acoustic wave heating of Fawzy et al. (2002b) (dashed line in Fig. 3), both in absolute magnitude (within a factor of about 1.5) and in terms

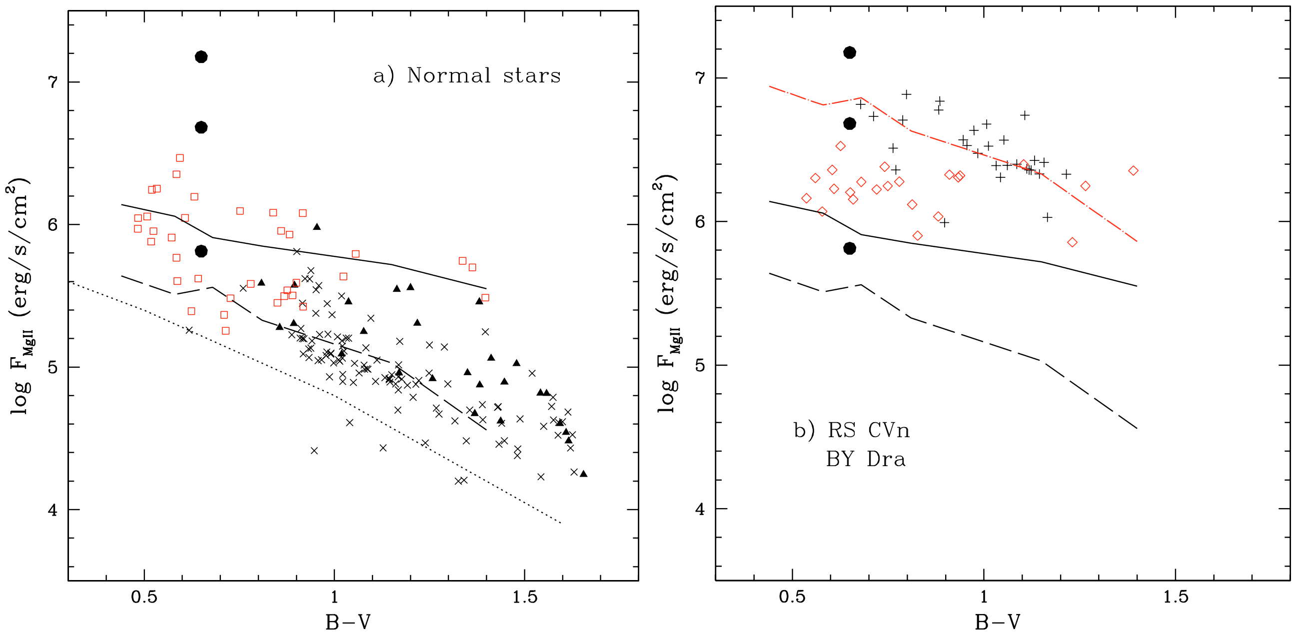

Fig. 3. The logarithm of the observed surface flux in the Mg II *k* line is plotted as a function of $B-V$. **a)** Quiet stars. Dwarfs are shown as open squares, class III–IV stars as crosses and class I–II stars as triangles. **b)** BY Dra stars (diamonds) and RS CVn (pluses). Also shown in each panel are the theoretical fluxes for pure acustic wave heating (dashed) and for magnetic wave heating in flux tubes (solid) as given by Fawzy et al. (2002b; Fig. 11) and corrected to consider the *k* line only. The dotted line in panel **a)** represent the observational minimum limits by Rutten et al. (1991). The dash-dotted line in panel **b)** is the theoretical flux for pure acustic wave heating increased by 1.3 dex.

of temperature dependence. At higher temperatures, where only main sequence stars are present, the minimum flux levels are less well defined, but they are still compatible with the theoretical lower limit. Note that the present minimum fluxes lie above the limit given by Rutten et al. (1991). Class I–II stars emission fluxes are greater than that of class III stars. This fact, not caused by magnetic heating, is probably due to their lower surface gravity.

In our sample of "normal" stars, the maximum values of Mg II fluxes are observed in main sequence stars. If, as said before, dwarf and giant stars have the same lower boundary, then the spread of Mg II fluxes in the vertical direction is larger for dwarfs than for giants stars (not considering supergiants). This means that dwarfs may have a range of activity levels greater than giants of the same spectral type. We can see that 60% of normal main sequence stars lie below the theoretical magnetic wave heating line and all but one lie below the theoretical upper limit if a factor of two uncertainty is taken into account. Evidently a large fraction of the atmosphere of dwarfs may be dominated by magnetic heating but their emission can be accounted for by present models.

On the contrary the cited two-component models seem to be inadequate to explain the observed chromospheric radiative loss rates of BY Dra and RS CVn stars.

Fawzy et al. (2002a) models describe correctly the chromospheres of solar-type stars with low and moderate levels of activity. In addition their models are based on uniformly distributed magnetic flux tubes. BY Dra stars are generally attributed deep convection zones and fast rotation rates that enhance magnetic activity and it is known that BY Dra stars have large spotted regions (Stewart et al. 1988; Baliunas & Vaughan 1985; Saar et al. 1992).

In our data shown in Fig. 3b, the BY Dra stars have Mg II fluxes which show no dependence on temperature, and they all lie above the line of magnetic wave heating (full line) with a mean value of 6.3 erg cm^{-2} s^{-1} (see also Sect. 4.1). Looking at the data relative to the Sun reported in Fig. 3, the value of 6.3 corresponds, following an empirical computation, to a fraction of stellar surface covered by plages of about 32%, if the brightness of typical solar plages is assumed (it is not excluded however that the intrinsic brightness of the plage regions exceeds that of typical solar plages) (Cerruti-Sola et al. 1992). Perhaps stronger magnetic fields and a modeling different from magnetic flux tubes are necessary to account for the peculiarities of this kind of star.

Figure 3b also shows that RS CVn stars lie far above normal-chromosphere stars (see also Fig. 1b). They seem to have a dependence on the effective temperature which follows the slope of the *basal* flux enhanced by a factor as large as 20 (dash-dotted line in Fig. 3b). However this feature may be simulated by different orbital periods. These chromospherically active stars are members of binary systems and interactions between the two components could produce excess heating by completely non-magnetic processes such as mass transfer and accretion, tidal interactions and resonances. These other physical processes could affect chromospheric activity in addition to magnetic field strength (see for example Glebocki & Stawikowski 1988).

6. Conclusion

In this paper we have addressed the still unsolved problem of identifying the possible physical processes responsible for chromospheric heating. To this purpose we have measured intensities of the Mg II *k* line in a large number of *IUE* spectra and we have carried out an analytical study for different types of stars. The results obtained can be summarized as follows:

- Metallicity does not affect the emission flux level of the Mg II *k* line.
- The logarithm of the total *k* line emission luminosity is linearly related to the absolute visual magnitude. For evolved stars, both normal and RS CVn, the correlation is very strong and allows the linear relationships in Eqs. (2) and (4) to be defined. Main sequence stars, both normal and BY Dra, are less correlated in the (M_V, log $L_{\mathrm{Mg\,II}}$) plane and show a smaller slope.
- There are indications that the Mg II *k* flux increases slowly with decreasing stellar gravity (supergiants).
- The observed range of chromospheric activity in the Mg II *k* line in normal stars is fully accounted for by current models based on acoustic and magnetic wave heating in the form of magnetic flux tubes.
- Peculiar objects, like BY Dra and RS CVn, for which current models are inadequate to explain the very large strength of the Mg II *k* line, require that additional heating processes be taken into account.

Acknowledgements. The author is grateful to Dr. A. Cassatella for providing measurements of Mg II *k* line intensities and for critically reading the manuscript. I thank the referee for useful comments and suggestions.

References

Allen, C. W. 1983, Astrophysical Quantities (London: Athlone Press, 1983)
Ayres, T. R. 1979, ApJ, 228, 509
Baliunas, S. L., Vaughan, A. H. 1985, ARA&A, 23, 379
Baliunas, S. L., Donahue, R. A., Soon, W. H., et al. 1995, ApJ, 438, 269
Basry, G. S., & Linsky, J. L. 1979, ApJ, 234, 1023
Buchholz, B., Ulmschneider, P., & Cunz, M. 1998, ApJ, 494, 700
Cardini, D., Cassatella, A., Badiali, M., Altamore, A., & Fernández-Figueroa, M. J. 2003, A&A, 408, 337
Carney, B. W., Latham, D. W., Laird, J. B., & Aguilar, L. A. 1994, AJ, 107, 2240
Cassatella, A., Altamore, A., Badiali, M., & Cardini. D. 2001, A&A, 374, 1085
Cayrel de Strobel, G., Soubiran, C., Friel, E. D., Ralite, N., & Francois, P. 1997, A&AS, 124, 299
Cerruti-Sola, M., Cheng, C.-C., & Pallavicini, R. 1992, A&AS, 256, 185
Cutispoto, G. 1998, A&AS, 131, 321
Cutispoto, G., Messina, S., & Rodonò, M. 2003, A&A, 400, 659
Elgarøy, Ø., Engvold, O., & Jorås, P. 1997, A&A, 326, 165
Fawzy, D., Rammacher, W., Ulmschneider, P., Musielak, Z. E., & Stepień, K. 2002a, A&A, 386, 971
Fawzy, D., Ulmschneider, P., Stepień, K., Musielak, Z. E., & Rammacher, W. 2002b, A&A, 386, 983
Fekel, F. C., Strassmeier, K. G., Weber M., & Washuettl, A. 1999, A&AS, 137, 369
Flower, P. J. 1996, ApJ, 469, 355
Glebocki, R., & Stawikowski, A. 1988, A&A, 189, 199
Gray, R. O., Corbally, C. J., Garrison, R. F., McFadden, M. T., & Robinson, P. E. 2003, AJ, 126, 2048
Linsky, J. L., & Ayres, T. R. 1978, ApJ, 220, 619
Mathioudakis, M., & Doyle, J. G. 1992, A&A, 262, 523
Montes, D., De Castro, E., Fernández-Figueroa, M. J., & Cornide, M. 1995, A&AS, 114, 287
Narain, U., & Ulmschneider, P. 1996, Space Sci. Rev., 75, 453
Oranje, B. J., & Zwaan, C. 1985, A&A, 147, 265
Rutten, R. G. M., Schrijver, C. J., Lemmens, A. F. P., & Zwaan, C. 1991, A&A, 252, 203
Saar, S. H., Piskunov, N. E., & Tuominen, I. 1992, in Cool Stars, Stellar Systems, and the Sun, ASP Conf. Ser., ed. M. S. Giampapa, & J. A. Bookbinder, 26, 255
Schrijver, C. J. 1987, A&A, 172, 111
Stewart, R. T., Innis, J. L., Slee, O. B., Nelson, G. J., & Wright, A. E. 1988, AJ, 96, 371
Strassmeier, K. G., Rice, C. B., Fekel, F. C., & Scheck, M. 1993, A&AS, 100, 173
Ulmschneider, P., Fawzy, D., Musielak, Z. E., & Stepień, K. 2001, ApJ, 559, L167
Weber, M., & Strassmeier, K. G. 1998, A&A, 330, 1029
Weiler, E. J., & Oegerle, W. R. 1979, ApJS, 39, 537